MIMO Capacity Comparisons of Three Types of Colocated Dual-Polarized Loop Antennas

Dazhi Piao* and Lingyu Yang

Abstract—The 2×2 multiple-input-multiple-output (MIMO) capacities of three types of colocated dual-polarized loop (DPL) antennas with different current distributions and isolations are investigated in the free space (FS) channel, the corridor with perfect electric conductor walls (PEC corridor) and the corridor with concrete walls (CON corridor), separately. Capacity results show strong dependences on both the structure and the position of the DPL antenna, in addition to the propagation conditions. For all the three propagation scenarios, the largest capacity can be reached is in the PEC corridor, employing the DPL antenna with a uniform current distribution and a high isolation. Specifically, for a 20 dB signal-to-noise ratio (SNR), the maximum dual-polarized MIMO capacity is 13.1 bps/Hz, which is 1.97 time of that obtained by the one-polarized loop. It is also noted that, the rich-multipath environment can increase the robustness of the DPL MIMO system and the difference of the MIMO capacity obtained by different antenna structures will get smaller with respect to that in the FS channel.

1. INTRODUCTION

In the traditional polarization diversity systems, only two electric polarization components are exploited for two independent parallel channels by two orthogonal electric dipoles. Recently, multipolarized antennas based multiple-input-multiple-output (MIMO) systems have drawn a lot of research interests [1–7], due to their potential in the space limited MIMO applications. It has been proved to use multiple electric and magnetic polarization components to improve the channel capacity of wireless communication systems in some scattering environment by theoretical calculations and experiment measurements [6–9]. However, the multi-polarized MIMO system consisting of multiple colocated loop antennas are still not fully explored. In [9], we have designed a colocated dual-polarized loop antenna (DPL) which can be used to obtain two independent parallel channels. However, the factors affecting the capacity of the DPL MIMO systems are still not sufficiently investigated.

It is noticed that the current distribution and port isolation of the antennas are two crucial factors affecting the capacity of the multi-polarized MIMO system [4, 10]. Therefore, to further understand the relationship between these factors and the MIMO capacity, three types of the DPL antennas are selected with different current distributions and port isolations. The first type of DPL antenna is based on an ordinary loop, which has a nonuniform current distribution and a high isolation (NHL); the second type one has a uniform current distribution and a high isolation (UHL), which is based on a wideband horizontally polarized printed loop antenna [11], the third type (ULL) one has also a uniform current distribution but a low isolation, which is based on the Kandoian loop [12].

Apart from these inherent features of the antenna, the capacity of the multi-polarized MIMO system depends also on the propagation characteristics of the environment [1, 13]. Previous studies indicate that the multi-polarized MIMO system will have a large capacity in the rich-multipath environment

* Corresponding author: Dazhi Piao (piaodazhi@hotmail.com).
The authors are with the School of Information Engineering, Communication University of China, Beijing 100024, People's Republic of China.

and have the smallest capacity in the free space (FS) channel [6]. Thus, to test the performance of these DPL antennas in different application environments, three typical types of propagation conditions are selected, which are the FS channel, the corridor with perfect electric conductor walls (PEC corridor) and the corridor with concrete walls (CON corridor). The PEC corridor can imitate an extreme rich-multipath propagation environment for the infinite multiple reflections. The CON corridor is a more practical environment, but with fewer multipath compared with that in the PEC corridor, due to the effect of absorption.

2. ANTENNA STRUCTURE

The first type of antenna (NHL) consists of two simple printed loop antennas, as shown in Fig. 1. The basic geometry and the current distribution of the single loop antenna are shown in Fig. 2(a) and Fig. 2(b), respectively. As seen in Fig. 2(b), each loop has a non-uniform current distribution. Although colocated, the two loops still have a very high isolation, as shown in Fig. 3, the S_{12} and S_{21} are lower than $-55\,\mathrm{dB}$. Meanwhile the antenna has a wide bandwidth (2.1–3.7 GHz, for return loss less than $-10\,\mathrm{dB}$). If the working frequency is 2.4 GHz, the return loss S_{11} and S_{22} are about $-33\,\mathrm{dB}$, as presented in Fig. 3.

As seen in Fig. 2(a), the loop is printed on a Teflon substrate ($\varepsilon_r = 2.6$ and $\tan\delta = 0.002$) with a thickness $h = 0.5\,\mathrm{mm}$. The following is the specific parameters of the loop: outer radius $R_1 = 24.54\,\mathrm{mm}$, inner radius $R_2 = 16.64\,\mathrm{mm}$. The parallel strip length line acts as an impedance transformer $l_p = 14.24\,\mathrm{mm}$ width $\omega_p = 0.53\,\mathrm{mm}$ and a separation $g_p = 0.6\,\mathrm{mm}$. Then, adjusted by cutting out a gap between the parallel strip lines, one loop could allow for the insertion of another loop collocated and orthogonally.

As shown in Fig. 4, the UHL antenna consists also of two printed loop antennas, but with uniform current distributions. The basic geometry of the single unit is shown in Fig. 5(a) and its current distribution is shown in Fig. 5(b). The single loop is also printed on a Teflon substrate with a thickness $h = 0.7\,\mathrm{mm}$. The parameters of the loop is specified as following: inner radius $R_2 = 20.5\,\mathrm{mm}$, outer radius $R_1 = 24.11\,\mathrm{mm}$, angle of each line section $a_1 = 44°$, spacing angle between adjacent line section $a_2 = 1°$. In order to realize periodical capacitive loading, interlaced coupling lines are added at the end of each arc stripline section. Each interlaced coupling line has the following parameters: inner bulgy stub width $w_s = 1\,\mathrm{mm}$, separation $g_s = 0.4\,\mathrm{mm}$ between the inner bulgy stub and the outer hollow stub, angle $a_3 = 11°$ of the inner bulgy stub, and spacing angle $a_4 = 1°$ between the inner bulgy stub and the outer hollow stub. The loop antenna is fed by a parallel stripline whose length $l_p = 13\,\mathrm{mm}$, width $\omega_p = 0.5\,\mathrm{mm}$ and a separation of 0.8 mm acted as an impedance transformer.

For orthogonally colocating the two loops, each loop is cut out a gap whose width is 0.7 mm between the parallel strip lines. In Fig. 6, the scattering parameters of the UHL antenna are presented. It is clear that the return loss of the loop 1 and loop 2 (S_{11} and S_{22}) are below $-10\,\mathrm{dB}$ in the frequency band of 2.25–3.0 GHz. At the frequency of 2.4 GHz, the isolations are below $-40\,\mathrm{dB}$.
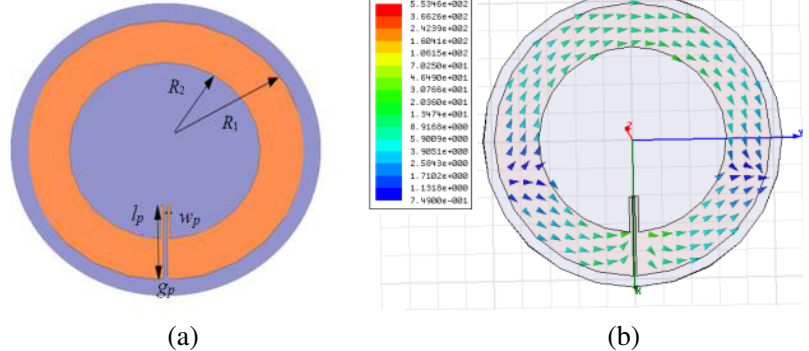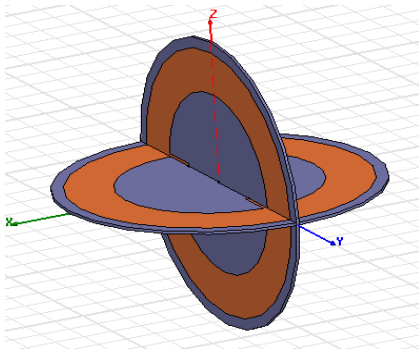
Figure 1. Geometry of the NHL antenna.

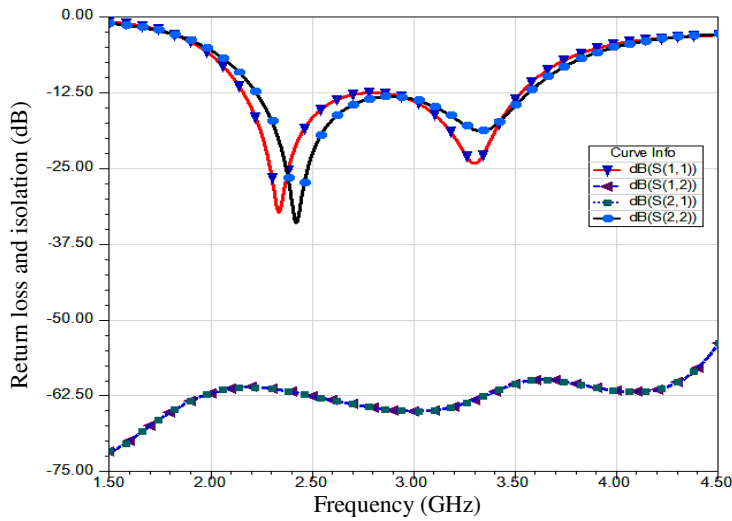**Figure 2.** The NHL unit. (a) Geometry. (b) Current distribution.
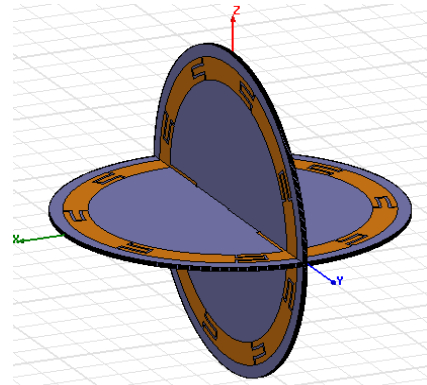
Figure 3. Return loss and isolation of NHL.

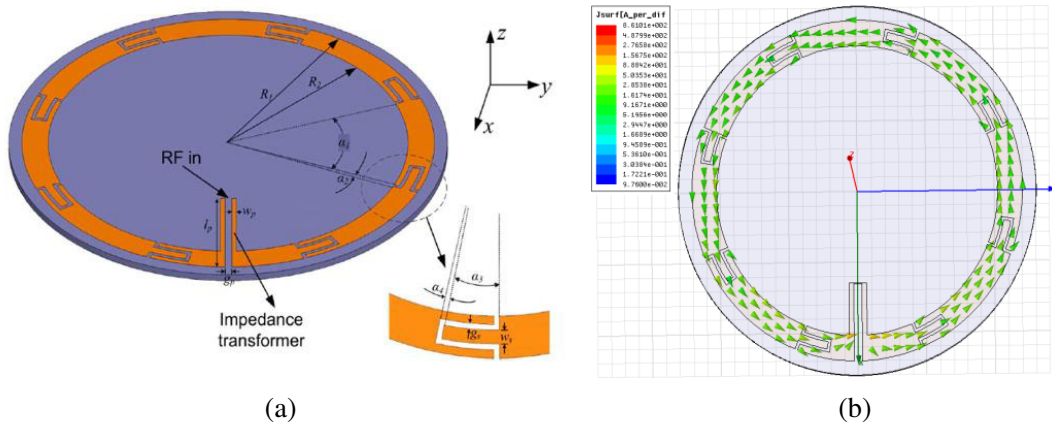**Figure 4.** Geometry of the UHL antenna.

(a)

(b)

Figure 5. The UHL unit. (a) Geometry. (b) Current distribution.

As shown in Fig. 7, the third kind of antenna is also composed of two printed loops with constant current distributions. But the two loops have a comparatively high mutual coupling.

The electric loop is printed on a Rogers 4003 substrate ($\varepsilon_r = 3.38$) with a thickness $= 1.5$ mm, board dimensions 90 cm. After the optimization, the following parameters of this antenna are determined: radius of loop $= 28.5$ mm, 2-mm-wide traces; bottom ground arms $= 17$ cm $\times$ 17 cm and top ground patch $= 4$ cm $\times$ 4 cm. The ULL is based on the Kandoian loop [12]. Fig. 8 illustrates the basic geometry and the current distribution of the single one, which is constructed as a two-layer printed circuit board. The top level (layer 1) is the loop itself, and the bottom level (layer 2) is the ground plane. A coaxial connector connected to the second layer which also encompasses the connector ground is used to feed this antenna. Each loop is also modified by slots and gaps to orthogonally colocate them. After colocating, the S-parameters of the ULL are illustrated in Fig. 9, which shows that at the frequency of 2.4 GHz, the values of the return loss of the loop 1 and loop 2 (S_{11} and S_{22}) are about -15 dB.
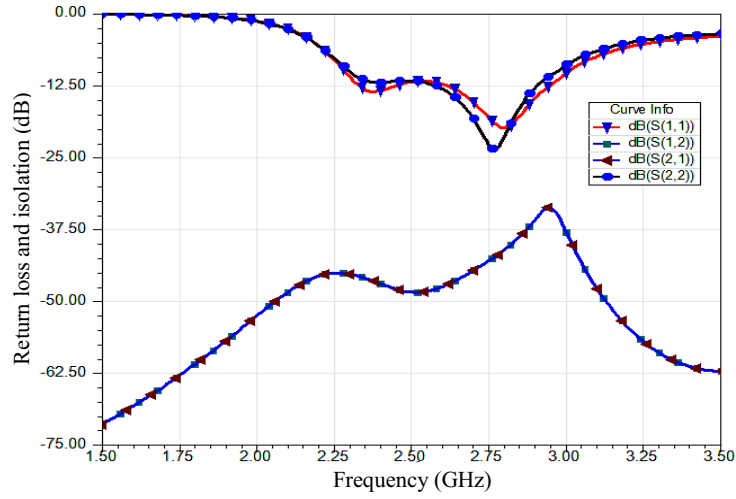
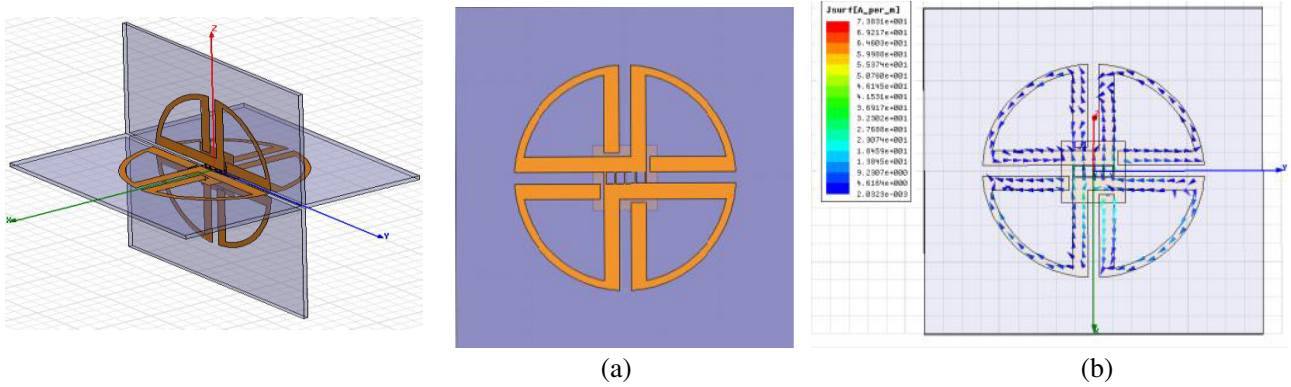**Figure 6.** Return loss and isolation of the UHL.

(a)   (b)

Figure 7. Geometry of the ULL antenna.

Figure 8. The ULL unit. (a) Geometry. (b) Current distribution.
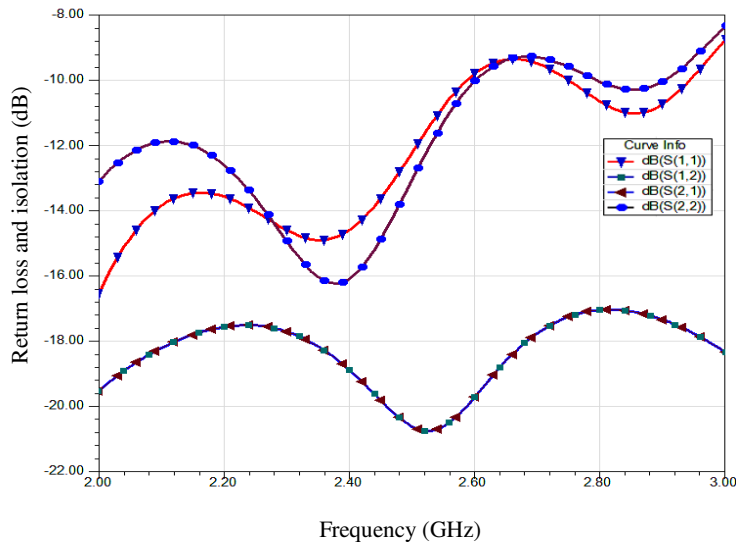

Figure 9. Return loss and isolation of ULL.

3. RESULT AND DISCUSSION

Channel capacity is defined as the highest achievable bit rate of information that can be sent with arbitrary low probability of error. The capacity of the MIMO system is computed by [13]

$$\mathbf{C} = \log_2 \det(\mathbf{I} + (SNR \ /n_T)\mathbf{HH}^+), \tag{1}$$

where $\mathbf{I}$ is the $n \times n$ identity matrix, $n_T = 2$ and SNR is the average signal-to-noise ratio at each receive element. The evaluation of the channel capacity is performed with 20 dB SNR in this paper, $\mathbf{H}^+$ means the transpose conjugate of $\mathbf{H}$, and $\det(\cdot)$ is the matrix determinant. In order to remove the effect of the total received power for a given computation, we adopt a widely used channel normalization that $\|\mathbf{H}\|_F = n_T \times n_R$, where $\|\cdot\|_F$ denotes the Frobenius norm.

The construction of the 2×2 MIMO channel matrix in this paper is shown as follows. Considering the transmit antenna configuration shown in Fig. 10, Tx_1 is located on the x-z plane, whose axis is along the y axis; Tx_2 is located on the x-y plane, whose axis is along the z axis. For each transmitting loop, 3 magnetic field components can be obtained Hx, Hy, and Hz, which are illustrated in Fig. 11 (The free space channel) and Fig. 12 (The PEC corridor channel). We find that the maximum capacity could be obtained if the field components corresponding to the polarizations of the transmit antennas are employed.
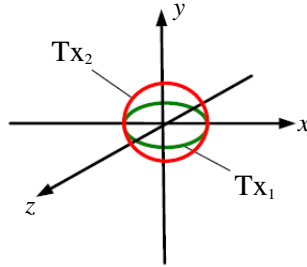

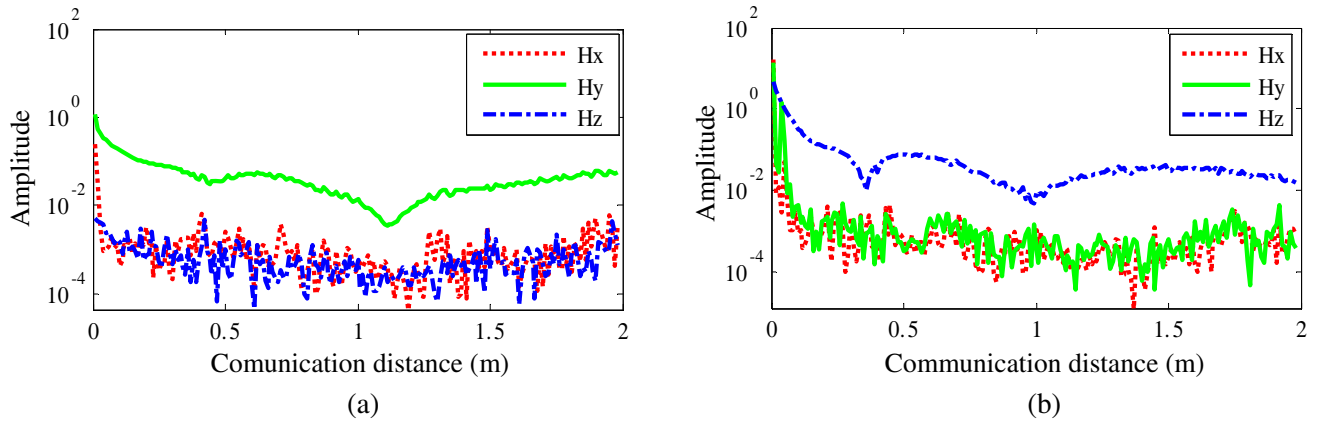**Figure 10.** Configuration of the dual-polarized antenna.

Figure 11. Magnetic field component in the FS. (a) Tx_1. (b) Tx_2.

In particular, for the channel matrix $\mathbf{H} = \begin{bmatrix} h_{11} & h_{12} \\ h_{21} & h_{22} \end{bmatrix}$, h_{11} and h_{21} are the y and z magnetic field components produced by Tx_1 correspondingly and h_{12} and h_{22} are the y and z magnetic field components produced by Tx_2 correspondingly.

To investigate the effect of propagation environment on the performance of these DPL antennas, these antennas are applied in the afore-mentioned three typical propagation environments including FS, PEC corridor and CON corridor, individually. The distance between the Tx and Rx antennas is from
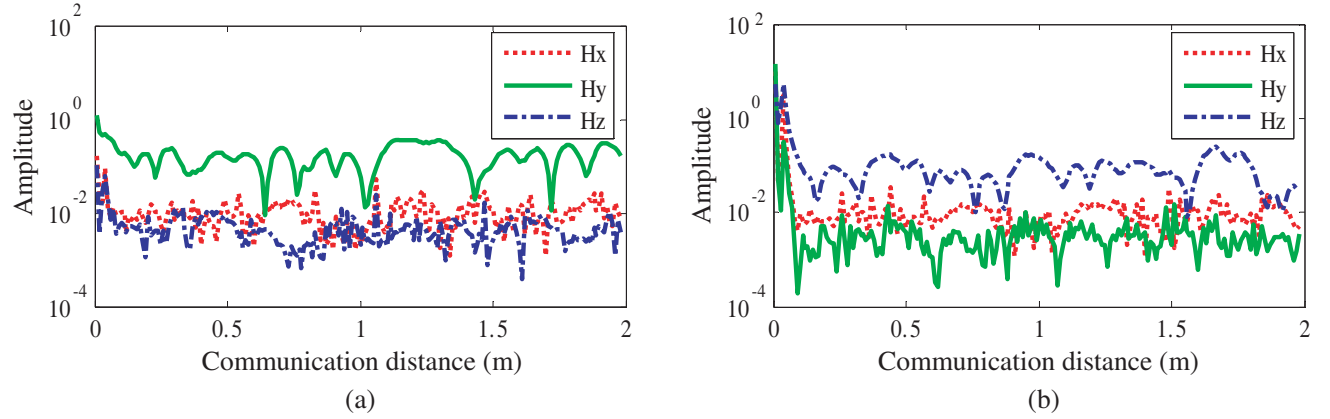
Figure 12. Magnetic field component in the PEC corridor. (a) Tx_1. (b) Tx_2.
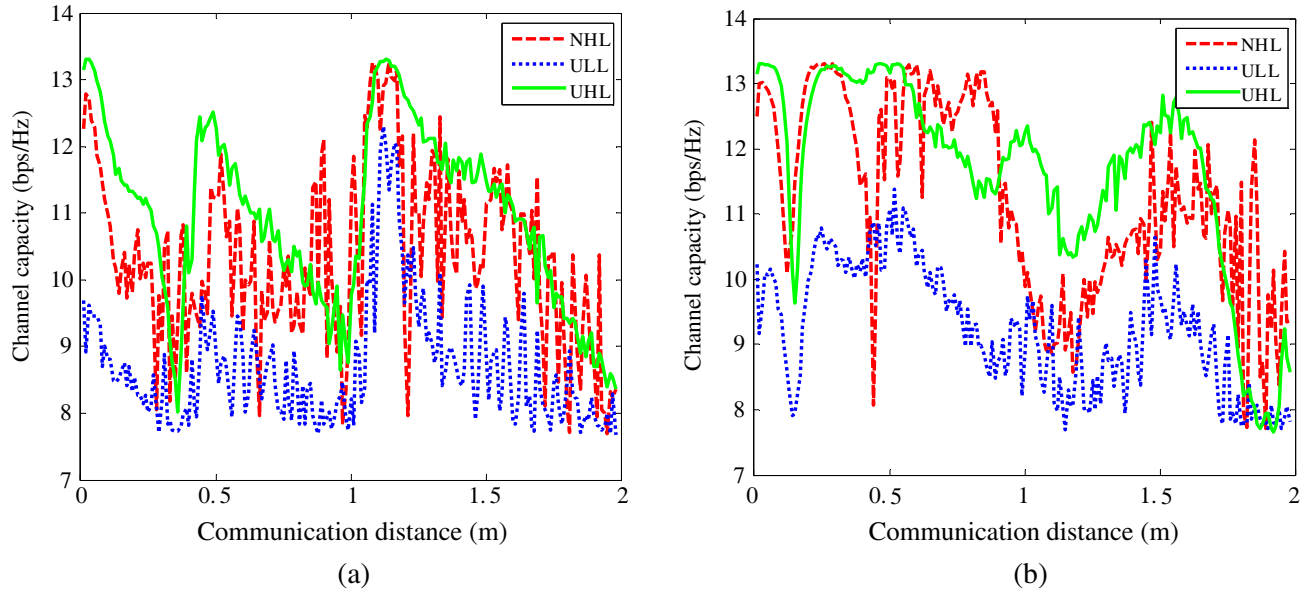
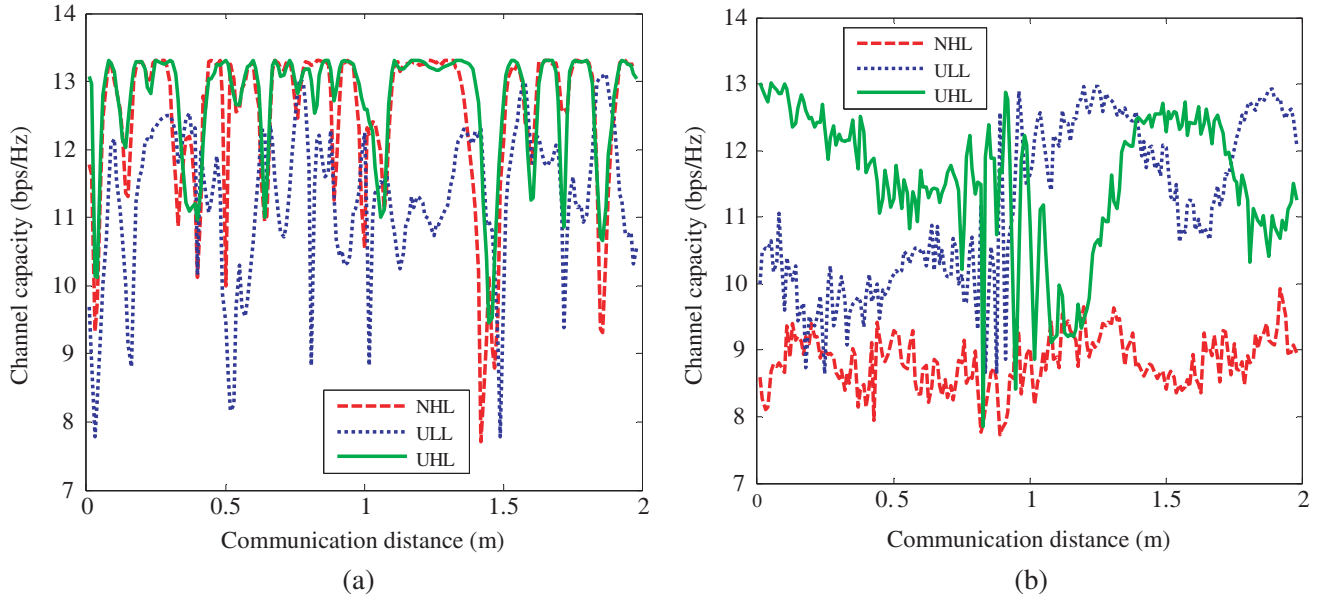**Figure 13.** Capacity of the FS. (a) $h_r = 30$ cm. (b) $h_r = 10$ cm.

0.03 m to 2 m. Meanwhile, the height of the Tx antenna h_t is kept as a constant of 30 cm, and two heights of the Rx antenna h_r are selected, the first one is 30 cm, and the second one is 10 cm. Thus the effects of antenna height on the characteristics of the DPL MIMO channels can be illustrated.

In Fig. 13, the capacity performances of the three types of DPL antennas in FS are illustrated. Fig. 13 shows that in FS, there is a big difference in the dual-polarized MIMO (DPM) capacity if different structures of antenna are used. It is seen that, for the same Tx and Rx antenna heights, the largest and the smallest capacity is obtained by the UHL and the ULL, respectively. The capacity obtained by the UHL antenna could be 20 percent larger than that of the ULL antenna. For different Tx and Rx antenna heights, the UHL and the ULL have similar capacities, which are about 30 percent larger than that of the NHL.

In Fig. 14 and Fig. 15, the capacity of the DPL antennas in the PEC corridor and the CON corridor are investigated, individually. Due to the computational limitations, the dimensions of the corridors are selected as 2.4 m (length) × 0.8 m (width) × 0.8 m (height). The thickness of the walls in the CON corridor is 20 mm.

Figure 14 shows that in the PEC corridor, which is a fully-scattered environment, the capacity of the DPM is obviously larger than that in the FS channel. In Fig. 14(a), it is seen that both the UHL and the NHL can obtain large MIMO capacities, which are larger than 13 bps/Hz and close to the limit capacity (for 20 dB SNR, the capacity of the one-polarized loop system is 6.65 bps/Hz, computed by

Figure 14. Capacity of the PEC corridor. (a) $h_r = 30$ cm. (b) $h_r = 10$ cm.
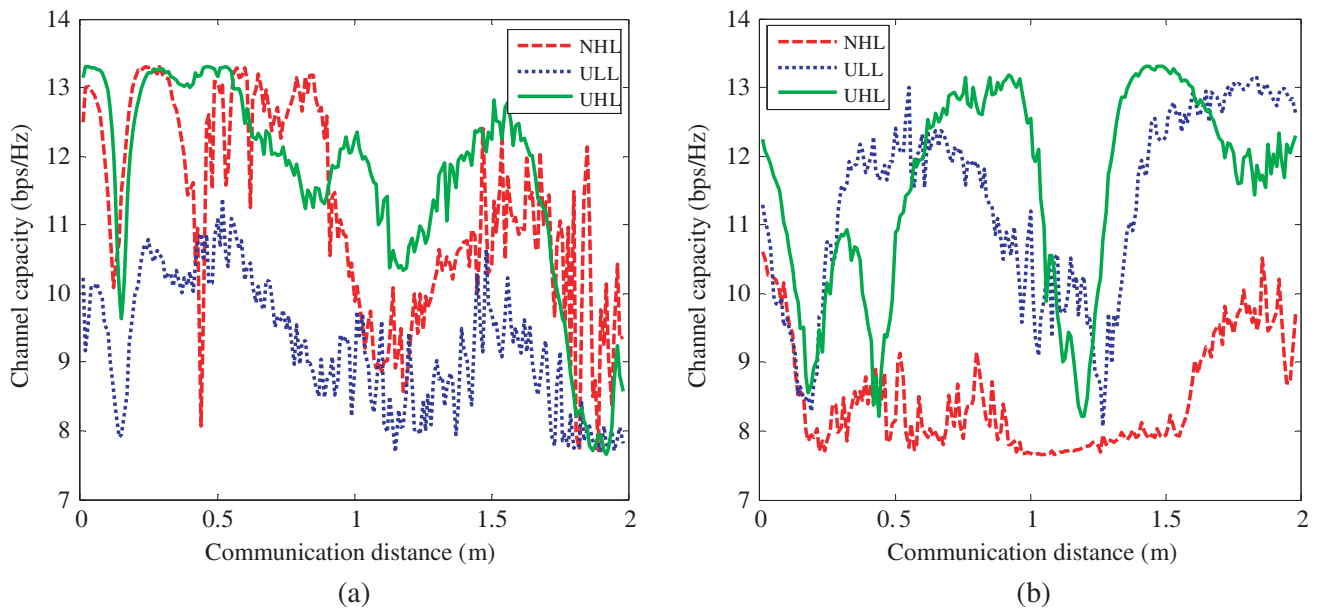
Figure 15. Capacity of the CON corridor. (a) $h_r = 30$ cm. (b) $h_r = 10$ cm.

the Shannon theorem. 6.65 bps/Hz $\times 2 = 13.3$ bps/Hz) of the DPM system. Furthermore, the average capacity of the ULL is also increased about 20 percent with respect to that in the FS. But in Fig. 14(b), the capacity acquired by the NHL is 25–35 percent less than that of the other two antennas.

As seen in Fig. 15 that, for the same Tx and Rx antenna heights, the capacity of the DPM in the CON corridor will be larger than that in the FS but be smaller than that in the PEC corridor. In these three scenarios, the capacities of the UHL and the NHL have the similar results, but the capacity of the ULL shows great differences. It gets the largest value in the PEC corridor, which is about 12 bps/Hz, and gets a smaller value in the CON corridor, which is about 10 bps/Hz, and gets the smallest one in FS, which is 8.5 bps/Hz. But for different Tx and Rx antenna heights, these three types of the DPL antennas have similar capacities in the three propagation environments.

Evidently, for all of the scenarios mentioned above, using the UHL antenna, which has a constant current distribution and a high isolation can obtain the largest capacities, which is near 2 times of that

obtained by the OPL. Furthermore, for each given type of the DPL antenna, the maximum capacities can be obtained in the PEC corridor.

4. CONCLUSIONS

In this paper, the effects of current distribution and port isolation of DPL on the DPM channel capacity are investigated in three propagation environments. Computation results show that besides the propagation conditions, the structure and position of the DPL antenna also have strong effects on the performance of the DPM system. Specifically, when the Tx and Rx antennas are located at the same height, both the UHL and NHL antennas can reach a high capacity in all the three scenarios, and the capacity of the ULL antenna can be greatly increased in the PEC corridor with respect to that in the FS. When the Tx and Rx antennas are not with the same height, the performances of the three types of DPL antennas do not show great differences in the three propagation environments. On the whole, the DPL antenna with a uniform current distribution and a high port isolation always presents a large DPM capacity. More structures of multi-polarized antennas with different current distributions and port isolations will be designed and measured in the future.

ACKNOWLEDGMENT

REFERENCES

1. Poon, A. S. Y. and D. N. C. Tse, "Degree-of-freedom gain from using polarimetric antenna elements," *IEEE Trans. Inf. Theory*, Vol. 57, No. 9, 5695–5709, Sep. 2011.
2. Ren, J., D. Mi, and Y. Yin, "Compact ultra-wideband MIMO antenna with WLAN/UWB bands coverage," *Progress In Electromagnetics Research C*, Vol. 50, 121–129, 2014.
3. Stancil, D., A. Berson, J. P. V. Hof, R. Negi, S. Sheth, and P. Patel, "Doubling wireless channel capacity using co-polarized, co-located electric and magnetic dipoles," *Electron. Lett.*, Vol. 38, No. 5, 746–747, Jul. 2002.
4. Ni, W. and N. Nakajima, "Experimental study on the capacity of compact MIMO antennas for portable terminals," *Wireless Personal Commun.*, Vol. 58, 439–453, 2011.
5. Varzakas, P., "Average channel capacity for rayleigh fading spread spectrum MIMO systems," *International Journal of Communication Systems*, Vol. 19, No. 10, 1081–1087, Dec. 2006.
6. Andrews, M. R., P. P. Mitra, and R. De Carvalho, "Tripling the capacity of wireless communications using electromagnetic polarization," *Nature*, Vol. 409, 316–318, 2001.
7. Elnaggar, M. S., S. K. Chaudhuri, and S. Safavi-Naeini, "Multi-polarization dimensionality of multi-antenna systems," *Progress In Electromagnetics Research B*, Vol. 14, 45–63, 2009.
8. Piao, D., "Characteristics of the hexapolarized MIMO channel over free-space and three non-free-space scenarios," *IEEE Trans. Wireless Commun.*, Vol. 12, No. 8, 4174–4182, Aug. 2013.
9. Piao, D., Y. Mao, and H. Zhang, "Two novel colocated dual-polarized antennas with extremely low mutual coupling for polarization diversity MIMO applications," *Proc. The 2nd International Conference on Connected Vehicles & Expo (ICCVE 2013)*, Las Vegas, USA, Dec. 2–6, 2013.
10. Recioui, A. and H. Bentarzi, "Capacity optimization of MIMO wireless communication systems using a hybrid genetic-taguchi algorithm," *Wireless Personal Commun.*, Vol. 71, 1003–1019, 2013.
11. Wei, K., Z. Zhang, and Z. Feng, "Design of a wideband horizontally polarized omnidirectional printed loop antenna," *IEEE Antennas Wireless Propag. Lett.*, Vol. 11, 49–52, 2012.
12. Elnour, B. and D. Erricolo, "A novel colocated cross-polarized two-loop PCB antenna in the ISM 2.4-GHz band," *IEEE Antennas Wireless Propag. Lett.*, Vol. 9, 1237–1240, 2010.
13. Foschini, G. J. and M. J. Gans, "On the limits of wireless communications in a fading environment when using multiple antennas," *Wireless Pers. Commun.*, Vol. 6, No. 3, 311–335, 1998.